VOL. 118 NO. 9 SEP. 1992

ISSN 0733-9445
CODEN: JSENDH

Journal of Structural Engineering

AMERICAN SOCIETY OF CIVIL ENGINEERS

TRUCTURAL DIVISION

NONLINEAR MODELING OF TRUSS-PLATE JOINTS

By Leslie Groom[1] and Anton Polensek[2]

ABSTRACT: A theoretical model is developed for predicting mechanisms of load transfer between a wood member and a metal die-punched truss plate. The model, which treats a truss-plate tooth as a beam on an inelastic foundation of wood and applies Runge-Kutta numerical analysis to solve the governing differential equations, predicts the load-displacement trace and ultimate load of truss-plate joints. The model is verified with eight truss-plate joint types, three of which varied the number of teeth and five the plate and grain angle. Theoretical and experimental load-displacement traces show good agreement. Experimental traces show no significant difference between multiple teeth in rows and columns, indicating little stress interaction among teeth. The theoretical model accurately predicts the ultimate load and failure modes for complete joint test types, which vary with plate and grain geometry: teeth face bearing on end grain failed by tooth withdrawal or plate tensile failure, teeth edge bearing on end grain failed by plate peelback, and teeth bearing on side grain failed in wood perpendicular to grain.

INTRODUCTION

Light-frame wood trusses are extensively used for supporting roofs and floors in the construction of residential, commercial, and farm buildings. Truss joints usually consist of light-gauge steel plates with die-punched teeth. An accurate model of stress transfer and deformations within the joint must account for nonlinear orthotropic behavior of such variables as tooth crushing of wood and frictional resistance of a tooth to an applied lateral load.

Kuenzi (1953) was the first to apply beam-on-elastic-foundation theory to model laterally loaded joints with connectors such as bolts and nails. He applied solutions of Hetényi (1946) and considered a connector as a beam supported by wood acting as an elastic foundation. Although wood behaves linearly when compressed by small loads, it behaves nonlinearly in truss-plate joints due to the crushing of the wood during tooth penetration, necessitating modifications in Kuenzi's solution.

Wilkinson (1971) presented a theoretical analysis based on Kuenzi's work, which still had a linear foundation modulus but increased the degree of sophistication for nailed joints by using polynomial functions to represent nonlinear slip between wooden members. Foschi (1974) and Foschi and Bonac (1977) modeled the load-slip characteristics of joints nailed with predrilled steel plates, commonly used in the 1970s, by the finite-element method. His model included nail yielding and nonlinear modulus of wood foundation determined by nonlinear least-squares fit of experimental data. Foschi and Longworth (1975) presented a semianalytical, finite-element technique that predicted strength based on the failure of plate fasteners. In subsequent work on truss plates with die-punched teeth, Foschi (1977a,

[1]Res. Technologist, Southern Forest Exp. St., 2500 Shreveport Highway, Pineville, LA 71360; formerly, Res. Asst., Forest Res. Lab., Oregon State Univ., Corvallis, OR 97331.

[2]Prof. and Res. Engr., Forest Res. Lab., Oregon State Univ., Corvallis, OR.

Note. Discussion open until February 1, 1993. To extend the closing date one month, a written request must be filed with the ASCE Manager of Journals. The manuscript for this paper was submitted for review and possible publication on July 30, 1990. This paper is part of the *Journal of Structural Engineering*, Vol. 118, No. 9, September, 1992. ©ASCE, ISSN 0733-9445/92/0009-2514/$1.00 + $.15 per page. Paper No. 205.

1977b) treated plate joints as continuous systems and calculated slip values by an iterative virtual-work method, with the foundation modulus modified by Hankinson's formula for the varying angle between wood grain and plates. Foschi (1979) later incorporated this work into the analysis of entire truss systems.

Hirai (1983, 1985) and Tsujino and Hirai (1983) have recently developed numerical methods to solve beam-on-elastic-foundation equations of bolted wood joints with steel side members. They divided the curvilinear load-embedment curve into several linear sections and then solved the problem numerically by a stepwise linear analysis. An analogous approach could be used to describe truss-plate behavior.

The objective of this investigation was to develop a model for predicting the mechanism of force transfer between wood members and truss plates. The inputs are grain orientation and plate geometry, including orientation of the teeth, and material properties of connected members and plates. The outputs are joint slip and plate-tooth deformations for all loading regimes up to the ultimate load.

Theoretical Procedure

Model Description

The concept of beam-on-elastic foundation was selected as a basis in this study because of its successful use in modeling mechanical joints. Existing concepts were modified to account for: (1) Inelastic behavior of the tooth and wood foundation as it related to the bearing pressure and location along the tooth length; and (2) changing moment of inertia along the tooth length.

Material Properties

By allowing moment of inertia to vary along the tooth length, the model more accurately represents the actual tooth cross section. In addition, the possibility of plastic-hinge formation in the tooth is included at the tooth-plate connection where the maximum loading takes place.

The direction of the grain in the wood affects the load-embedment trace (Fig. 1). For a tooth bearing parallel to the grain, the trace generally has two linearly elastic regions joined by a small curvilinear section (Fig. 1) and can be represented by four linear regions associated with four deflection domains based on foundation moduli obtained from testing. For a tooth bearing perpendicular to grain, foundation moduli were obtained by a non-linear least-squares analysis of experimental data.

The inelastic behavior of the foundation modulus was accounted for by using a conventional step-by-step loading procedure, which involved sub-dividing the load acting on the tooth into small increments during which the joint was assumed to behave linearly. The linear responses were then evaluated and accumulated for each increment.

Governing Differential Equations

In a typical truss-plate tooth under lateral load, P = the load transferred through the joint, M is caused by the resistance of the tooth to rotate about the point of its attachment to the plate, and N = a withdrawal force that appears when the tooth and wood deform (Fig. 2). The resistance to P is dictated by the foundation modulus of wood, k, while N is resisted by the friction force with coefficient, μ.

The effect of N is included in the conventional equation for the beam on

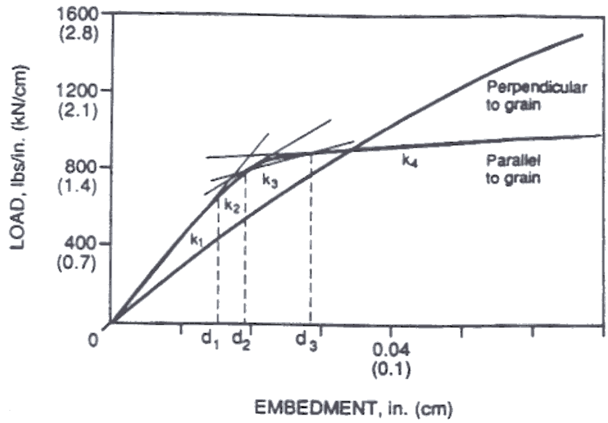

FIG. 1. Typical Load-Embedment Traces of Truss-Plate Tooth Flat-Bearing Parallel and Perpendicular to Grain

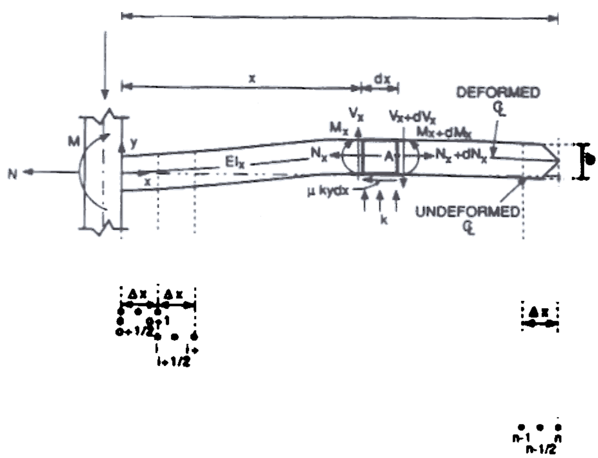

FIG. 2. Free-Body Diagram of Truss-Plate Tooth Bearing on Wood and Interval Identification for Numerical Analysis, Where P = Lateral Load, M = Restraining Moment, and N = Normal Load

elastic foundation as follows. Differentiation of the equilibrium equation between the frictional and withdrawal forces, $dN = \mu kydx$, gives

$$\frac{d^2N_x}{dx^2} = \mu k \frac{dy}{dx} \quad (1)$$

in which y = tooth deflection at point x (Fig. 2). Summing moments about point A of the free-body diagram in Fig. 2 and applying $EI(d^2y/dx^2) = -M$ gives the equation governing the equilibrium for flexural, withdrawal, and shear forces:

$$EI_x \frac{d^3y}{dx^3} - N_x \frac{dy}{dx} + V_x + \frac{\mu kb}{2} y + \frac{ky}{2} dx = 0 \quad (2)$$

in which E = tooth modulus of elasticity; I_x = tooth moment of inertia, which varies as a function of x; and v_x = shear force. Differentiation of (2) and substitution of (1) and the expressions $dV = kydx$ and $dN = \mu\, kydx$ into the resulting equation gives

$$\frac{d^4y}{dx^4} - \frac{N_x}{EI_x}\frac{d^2y}{dx^2} + \frac{ky}{EI_x} + \frac{\left(\frac{b}{2} - y\right)}{EI_x}\frac{d^2N_x}{dx^2} = 0 \quad \ldots\ldots\ldots\ldots\ldots\ldots (3)$$

Eqs. (1) and (3) are the two differential equations that govern the transfer of forces between the plate tooth and wood. The variables k and N are functions of y, which makes (3) a nonlinear differential equation for which a closed-form solution could not be found. As an alternative, the two equations were solved numerically by a Runge-Kutta analysis.

Boundary Conditions

During initial stages of analysis, the boundary conditions of the tooth are those of a rigid cantilever beam on an elastic foundation with slope equal to zero at the tooth-plate interface. However, when M exceeds the yield moment of the tooth, the boundary conditions are modified to allow tooth rotation while applying a constant moment, thus simulating the formation of a plastic hinge at the tooth support. The starting boundary conditions are: $N(0) = N$, $N(L) = 0$, $dy/dx(0) = 0$, $d^3y/dx^3(0) = -P/EI$, $d^2y/dx^2(L) = 0$, and $d^3y/dx^3(L) = 0$. After the hinge formation, the tooth is allowed to rotate about its base. This rotation is restrained by a moment equaling 1.5 times the yield moment, thus behaving as a rotational spring. The value of 1.5 times the yield stress was chosen as the plastic hinge origin to allow the hinge to spread throughout its rectangular cross section (Beedle 1958).

The frictional forces in the model act on the three sides of the tooth that remain in intimate contact with the wood throughout loading. The two nonbearing tooth sides have constant frictional forces that are a function of the tooth width. The bearing surface of the tooth has a frictional force proportional to the absolute value of the lateral deflection. The nonbearing topside of the tooth is generally not in contact with the wood during loading and thus is assigned no frictional force.

Numerical Solution

Fig. 2 illustrates the subdivision of tooth length into intervals of length, Δx, within which material and geometric properties are constant. Runge-Kutta analysis projects current estimates for solutions at the end of the ith interval from values of the previous estimate, $i - 1$ until all n intervals have been accounted for. Several types of Runge-Kutta analyses exist, but this study developed from the following fourth-order coefficient (Hornbeck 1975):

$$y_j^{(i+1)} = y_j^{(i)} + \Delta x \left\{\frac{1}{6} f(y_j^{(i)}, x^{(i)}) + \frac{1}{3} f[q_1^{(i+1/2)}, x^{(i+1/2)}]\right.$$

$$\left. + \frac{1}{3} f[q_2^{(i+1/2)}, x^{(i+1/2)}] + \frac{1}{6} f[q_3^{(i+1)}, x^{(i+1)}]\right\} \qquad (j = 1, 2, \ldots, 6) \ldots (4)$$

in which y_1 = tooth displacement; y_2 = tooth slope; y_3 = moment; y_4 = shear; y_5 = frictional force between tooth and wood; and y_6 = frictional rate of change along tooth length, $q_1^{(i+1/2)} = y_j^{(i)} + \Delta x/2\ f[y_j^{(i)}, x^{(i)}]$,

$q_2^{(i+1/2)} = y_j^{(i)} + \Delta x/2\, f[q_1^{(i+1/2)}, x^{(i+1/2)}]$, and $q_3^{(i+1)} = y_j^{(i)} + \Delta x\, f[q_2^{(i+1/2)}, x^{(i+1/2)}]$. Calculations for intermediate coefficients q_1, q_2, and q_3 proceed from the previous estimate, i, along Δx to the interval midpoint, $i + 1/2$, and finally to the interval terminus where the current estimate is calculated at $i + 1$ (Fig. 2), until n tooth intervals have been accounted for.

Runge-Kutta analysis is limited to initial-value, first-order linear or nonlinear differential equations, so (1) and (3) were transformed into six equivalent first-order differential equations:

$$\frac{dy_1}{dx} = y_2 \quad \ldots\ldots (5)$$

$$\frac{dy_2}{dx} = y_3 \quad \ldots\ldots (6)$$

$$\frac{dy_3}{dx} = y_4 \quad \ldots\ldots (7)$$

$$\frac{dy_5}{dx} = y_6 \quad \ldots\ldots (8)$$

$$\frac{dy_4}{dx} = \frac{1}{EI}\left[y_5 y_3 - k y_1 - \left(\frac{b}{2} - y_1\right) y_6\right] \quad (9)$$

$$\frac{dy_6}{dx} = \mu k y_2 \quad \ldots\ldots (10)$$

The unknown initial values, $y(0)$, $d^2y/dx^2(0)$, and $dN/dx(0)$, must be determined from the boundary conditions, $d^2y/dx^2(L)$, $d^3y/dx^3(L)$, and $N(L)$, respectively. Runge-Kutta solutions for the nth interval are compared to the aforementioned boundary conditions. If agreement between the boundary conditions and Runge-Kutta solutions is not within tolerance, new initial-value estimates are determined from a Newton-Raphson technique (Hornbeck 1975), which include partial derivatives of deformations at the tooth end. This analysis gives the values of deflection and its derivatives at any location along the tooth. Boundary conditions, material properties, and loading regimes can be easily altered, and their effect on the model studied.

Failure Criteria

Single-Tooth Joint

The theoretical maximum load a single-tooth joint could withstand was defined as the lateral load at which tooth withdrawal resistance was exceeded by the normal load caused by friction. Loading was applied incrementally with results accumulated. Normal load was taken as the product of tooth slope at the tooth-plate interface and lateral load. Withdrawal resistance was frictional resistance, as calculated from the Runge-Kutta analysis, integrated over tooth length. This failure mode was valid for all tooth orientations.

Complete Joint

The complexity of the failure mechanism increases when a full compliment of teeth is considered, with joint load being the cumulative load acting on

a tooth multiplied by the total number of teeth. Although tooth withdrawal is still a criterion for joint strength, the higher loads attained in complete joints result in higher stresses for the wooden members and truss plates than predicted by analyzing individual teeth because bearing stresses from one tooth spread over the adjacent teeth. These cumulative stresses from several teeth can be critical depending on tooth and grain orientation.

A failure criterion, based on wood strength, prevails when the grain angle is perpendicular to the applied loading. The ultimate load is based on a combination of tensile strength perpendicular to grain and rolling shear strength. As loading reaches the tensile strength perpendicular to grain, a crack results parallel to the grain at the perimeter of the truss plate. This crack significantly weakens the joint by transferring all stresses into an equivalent fixed-end moment beam of wood material pulled away from the wood section, with the length equal to crack length, depth equal to overlap length of the plate, and thickness equal to tooth length. The joint supports increasing loading until the rolling shear strength of the connecting wood is exceeded.

Another failure criterion relates to plate strength. The joint is assumed to fail when the tensile strength of the plate, based on the minimum plate cross-sectional area, exceeds its ultimate value. In yet another criterion, the plate is allowed to rotate when the cumulative moment acting on the outermost row of teeth exceeds the bending strength of the plate. This rotation allows the bottom row of teeth to withdraw from the wood and remaining teeth to carry the joint load. As loading is increased the next row of teeth is again allowed to rotate, resulting in additional plate rotation and transference of the load to yet fewer teeth. This process continues until all rows of teeth have peeled back, at which time the joint fails completely.

Elbow Joint

The array of truss plate teeth in the elbow joint is analyzed in a manner analogous to rivets in steel plates (Shigley 1977). The truss-plate center of rotation about each member is calculated by

$$\bar{x} = \frac{\sum_{1}^{n} k_m x_m}{\quad} \qquad (11)$$

$$\bar{y} = \frac{\sum_{1}^{n} k_m y_m}{\sum_{1}^{n} k_m} \qquad (12)$$

in which k_m = the foundation modulus of tooth m = y_m = associated tooth deformation. Individual k_ms are adjusted for varying grain and plate angle by Hankinson's formula. The centroid of each plate is determined for each iterative load step. The moment and shear loads acting on the truss plate of each member are distributed to each tooth based on the radial distances from the center of rotation to the center of each tooth. Joint deformation is then calculated from the corresponding tooth displacements, with failure occurring when the withdrawal resistance of the teeth is exceeded.

Computer Program

A program in Microsoft Fortran, called TRUSSCON, was written for the microcomputer. The inputs are material properties, friction coefficient tooth and grain orientations, tolerances for terminating iteration procedures, and loading specifications. The program evaluates the moment of inertia for each tooth segment before going into the actual analysis.

The primary subroutine calculates Runge-Kutta coefficients for each tooth interval, which are necessary to evaluate deflection and stresses. Deflection and stresses are accumulated in the main program with each incremented load. The main program also checks for joint failure and system convergence. Elbow joints are managed in a subroutine that determines the center of rotations about the truss plates, foundation modulus under each tooth, and overall joint displacement. For computational purposes, each tooth was divided into 10 intervals while the load was changed at 2-lb (0.9-kg) increments. Tolerances for the root estimates were 0.05% and 0.0005 in. (0.001 cm) for the displacement at the base of the tooth.

Procedure Accuracy

The accuracy of the developed procedure and program were verified by testing truss-plate joints and comparing observed and predicted results. Test specimens consisted of eight joint types with varying number of teeth, plate angle, and grain angle. Additional tests included those to determine formation modulus for tooth bearing and wood modulus of elasticity, which provided the input for the model analysis.

Experimental Procedure

Evaluation of Wood Properties

Experimental truss-plate joints were constructed from 11 boards with a wide range of specific gravities. Boards were Douglas fir, 2-by-4-in. *No. 1 and Better grade*, from two manufacturers in the upper Willamette Valley, Oregon, where this species and grade are typically used (Groom 1988).

Four different foundation moduli were determined for each board by embedment tests. The tooth was oriented either flat or on edge while the grain orientation was either parallel or perpendicular to the applied embedment load. A 1.5-in. (3.81-cm) metal cube, with two grooves for different tooth orientations, was clamped to a sample of wood. An individual tooth cut from a truss plate was completely driven into the wood at the wood-cube interface. The cube and the tooth were then removed, leaving a slight embedment mark, which simulated crushed wood from tooth driving. The 0.3-in.- (0.76-cm-) long loading head simulating a tooth oriented either on edge or flat was then forced into the embedment mark at a rate of 0.035 in./min (0.089 cm/min) until completely embedded. Three or four load-embedment traces, depending on the joint test type, were acquired for each board and appropriate tooth and grain orientation. The foundation modulus was then determined on the basis of the length and width of the embedment-loading head along with the average load-embedment trace for a given board and tooth and grain orientation (Tables 1 and 2).

Specific gravity and moisture content were measured on 1.5-in. (3.81-cm) wooden cubes taken from the joints after testing. Modulus of elasticity was determined in bending on 0.75-by-0.75-by-12-in. (1.91-by-1.91-by-30.48-cm)

TABLE 1. Parameters Defining Foundation Modulus for Teeth Bearing Parallel to Grain

Joint types (1)	Foundation type (2)	Board (3)	Foundation Moduli (MPa/mm)				Embedment Limit (mm)		
			k_1 (4)	k_2 (5)	k_3 (6)	k_4 (7)	d_1 (8)	d_2 (9)	
1, 2, 3	k_0	1	114	73.7	25.8	3.7	0.38	0.46	0.60
1, 2, 3	k_0	2	146	111	37.3	3.2	0.38	0.47	0.61
1, 2, 3	k_0	3	156	113	34.1	5.5	0.38	0.48	0.61
1, 2, 3	k_0	4	149	94.9	19.4	6.0	0.41	0.48	0.66
1, 2, 3	k_0	5	149	100	27.2	6.9	0.41	0.48	0.65
4, 5, 8 (diagonal)	k_0	6	135	91.7	32.3	5.5	0.37	0.48	0.67
4, 5, 8 (diagonal)	k_0	7	135	108	36.9	6.5	0.37	0.48	0.69
4, 5, 8 (diagonal)	k_0	8	152	117	36.9	3.2	0.34	0.52	0.69
4, 5, 8 (diagonal)	k_0	9	163	106	24.0	4.1	0.41	0.56	0.79
4, 5, 8 (diagonal)	k_0	10	159	99.1	24.0	4.1	0.41	0.56	0.79
4, 5, and 8 (diagonal)	k_{90}	6	93.9	59.8	34.1	11.0	0.53	0.74	0.97
4, 5, and 8 (diagonal)	k_{90}	7	89.0	57.3	34.1	4.9	0.66	0.79	0.93
4, 5, and 8 (diagonal)	k_{90}	8	93.9	69.5	30.5	7.3	0.55	0.86	1.04
4, 5, and 8 (diagonal)	k_{90}	9	111	76.8	42.7	7.3	0.46	0.65	0.93
4, 5, and 8 (diagonal)	k_{90}	10	105	73.2	35.4	8.5	0.48	0.74	1.22
8 (horizontal)	k_0	11	201	113	23.5	6.9	0.44	0.61	0.88

Note: k_i = foundation modulus for: $i = 0$, tooth bearing on face; and $i = 90$, tooth bearing on edge.

TABLE 2. Parameters Defining Foundation Modulus for Teeth Bearing Perpendicular to Grain

Joint types (1)	Foundation type (2)	Board (3)	A^* (4)	B^* (5)
6, 7, 8 (diagonal)	k_0	6	89.9	
6, 7, 8 (diagonal)	k_0	7	95.4	
6, 7, 8 (diagonal)	k_0	8	114	
6, 7, 8 (diagonal)	k_0	9	121	
6, 7, 8 (diagonal)	k_0	10	114	
6, 7, 8 (diagonal)	k_{90}	6	138	
6, 7, 8 (diagonal)	k_{90}	7	132	
6, 7, 8 (diagonal)	k_{90}	8	139	
6, 7, 8 (diagonal)	k_{90}	9	139	
6, 7, 8 (diagonal)	k_{90}	10	162	
8 (horizontal)	k_{90}	11	199	

Note: k_i = foundation modulus for: $i = 0$, tooth bearing on face; and $i = 90$, tooth bearing on edge. Foundation modulus: $k = A + 2Bd$ (A in MPa/mm, B in MPa/mm^2).

samples removed from the joints after testing. Coefficients of friction values were those obtained by Atherton (1982).

The die-punched truss plates in this study were made of 20-gauge grade C sheet metal, 3-in. (7.62-cm) wide and 4.5-in. (11.43-cm) long, with an average tooth density of 7.1 teeth/sq in. (1.10 teeth/cm^2). Average tooth width, effective thickness, and length were 0.087, 0.050, and 0.393 in. (0.127, 0.221, and 1.00 cm), respectively. Each tooth was theoretically divided into four regions of unequal length to account for changing dimensions along its length. Spacing between main columns was 0.50 in. (1.27 cm), with teeth from offset columns 0.25 in. (0.64 cm) apart. Row spacing was staggered at 0.42 in. (1.07 cm) and 0.14 in. (0.36 cm) apart.

Joint Construction and Testing

Of the eight joint types tested (Fig. 3), types 1–3 were constructed to discern the load sharing among the teeth in a row and among teeth in a column. Types 4–7 were constructed to evaluate the model's accuracy for varying tooth and grain angle. Type 8 tested the model's ability to analyze elbow joints. Epoxy adhesive was applied to the teeth of the upper member of each specimen to ensure failure in the lower member, which was equipped with displacement transducers. Adhesive was also applied to reduce slippage in the adhered portion of the joint, allowing a more precise measurement of displacements in joints tested. In accordance with Canadian Standards Association ("Methods" 1980), all teeth within 0.5 in. (1.27 cm) of the end and 0.25 in. (0.64 cm) of the edge were milled smooth. The joints were kept in a controlled hygrothermal environment for at least 72 hours to allow for relaxation of stresses induced by pressing.

The load was applied at a constant displacement rate of 0.025 in./min (0.0635 cm/min) such that failure occurred in 5–20 min. Load and deflection readings were acquired at a rate of two readings per second by a microcomputer with an automatic data-acquisition system.

The five boards used in joint types 1–3 needed only the foundation moduli for tooth-face bearing parallel to the grain. The six boards used for types

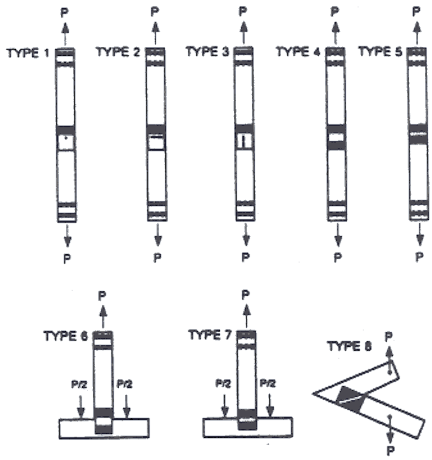

FIG. 3. Joint Types with Varying Number of Teeth (Type 1–3) and Different Plate and Grain Angles (Type 4–8)

4–8 needed all four foundation moduli: tooth-face and tooth-edge bearing parallel to the grain, and tooth-face and tooth-edge bearing perpendicular to grain. The load-embedment traces shown in Fig. 4 have been standardized by adjusting the foundation moduli to a fictitious 1-in. (2.54-cm) tooth length. The embedment data were prepared for the theoretical modeling by two methods: nonlinear regression and linearization. Load-embedment traces with teeth (flat and edge) bearing perpendicular to grain demonstrated a curvilinear behavior throughout the test [Fig. 4(*c*) and Fig. 4(*d*)]. For these traces, the following polynomial equation provided the best fit for nonlinear regression analysis:

$$P = Ad + Bd^2 \quad (13)$$

in which P = embedment load, d = deflection of tooth, and A and B = coefficients depending on test data. The foundation moduli were taken as the derivative of (13) at any given embedment and were adjusted for tooth width and length (Table 2).

The load-embedment traces with teeth (flat and edge) bearing parallel to the grain were linearized by dividing the traces into linear regions with corresponding deflection limits that defined the extent of their validity (Fig. 1).

Prediction Accuracy

Single Tooth

When theoretical and experimental traces of individual specimens for single-tooth, joint type 1 (Fig. 5) are compared, agreement is very close at low loads, and then the curves drift farther apart in the upper half of loading, but come closer again as the load reaches its ultimate value. At high loads, predictions are consistently above observed values, due to the change in geometry during the testing after some initial slip took place. Specifically, at low loads with very small slips, most of the load was transferred through the tooth. However, as slip increased and some withdrawal occurred, a

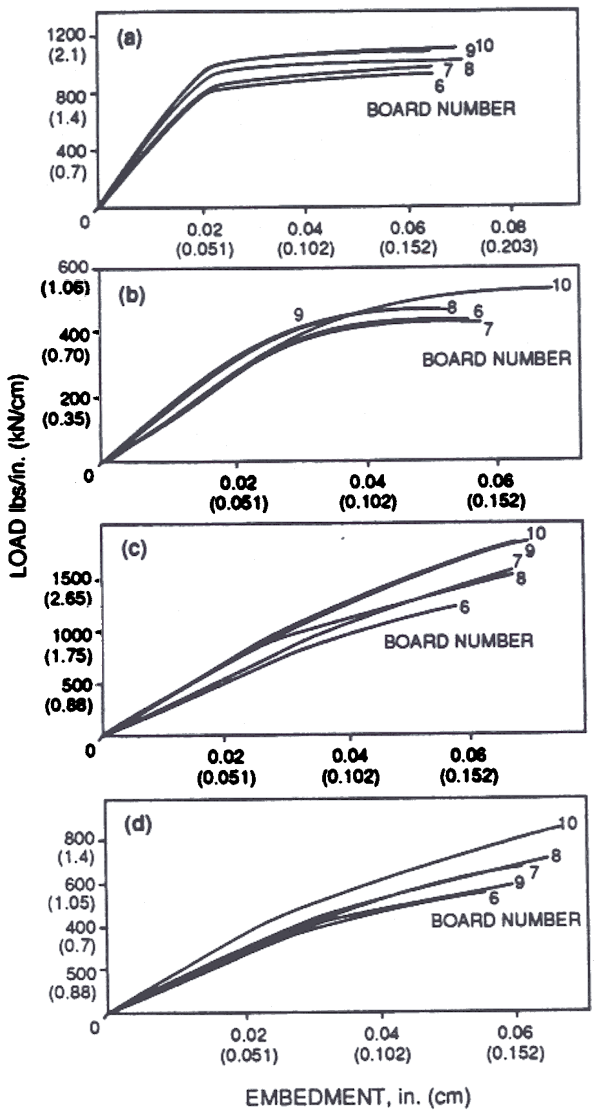

FIG. 4. Typical Load-Embedment Traces for: (*a*) Tooth Flat-Bearing Parallel to Grain; (*b*) Tooth Edge Bearing Parallel to Grain; (c) Tooth Flat-Bearing Perpendicular to Grain; (*d*) Tooth Edge-Bearing Perpendicular to Grain

compression contact developed between the toothless part of the plate and wood. This compression contact added another component to the tooth-withdrawal force, which accelerated the withdrawal and lowered the ultimate load. The difficulty of perfectly aligning the load through the tooth and contact surface between the toothless plate and wood also caused compression contacts and early withdrawal.

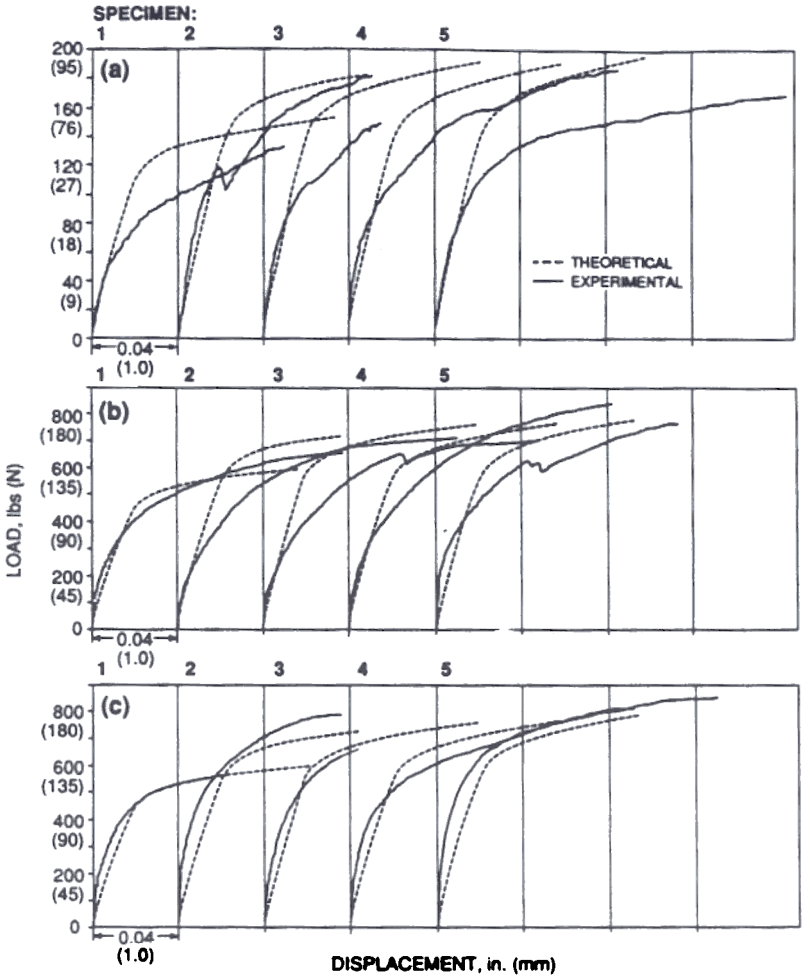

FIG. 5. Experimental versus Theoretical Traces of Slip for: (*a*) Single-Tooth Joint Type 1, and Multiple-Tooth Joint (*b*); Type 2; (c) Type 3

Multiple Teeth

No apparent difference exists in the general shape of the experimental data in Figs. 5(*a*), 5(*b*), and 5(*c*). This suggests a similar mode of failure in all 15 specimens, namely tooth withdrawal. For four-tooth traces, the theoretical results are very close to the observed values as the load approaches the ultimate value because the increased number of teeth minimize the compression contact that developed for a single tooth. The larger number of teeth kept the plate geometry from changing until near-failure loads were reached.

Table 3 shows the predicted and the experimental ultimate loads for joint types 1, 2, and 3. In type 3, the tooth furthest from the wood-wood juncture began withdrawing at approximately 80% of the ultimate load followed by the tooth next to it, resulting in a gradual withdrawal of all teeth at failure.

TABLE 3. Experimental and Theoretical Joint Failure per Tooth Loads and Mode of Failure

Specimen (1)	Type of failure loads (2)	Ultimate Load of Joint, N						
		Type 1[a] (3)	Type 2[a] (4)	Type 3[a] (5)	Type 4 (6)	Type 5 (7)	Type 6 (8)	
	Theoretical	309	309	309	370	330	212	211
	Experimental	296	366	306	358[b]	269[d]	202[e]	193[g]
2	Theoretical	394	394	394	370	319	217	218
2	Experimental	409	396	441	355[b]	325[d]	214[e]	210[g]
3	Theoretical	414	414	414	370	330	—	211
3	Experimental	334	394	371	366[c]	385[d]	—[f]	261[e]
4	Theoretical	407	407	407	—	341	217	211
4	Experimental	418	469	455	—[f]	310[d]	216[e]	210[g]
5	Theoretical	423	423	423	370	341	221[e]	218
5	Experimental	377	429	474	361[c]	377[d]	258[e]	259[g]
Average	Theoretical	389	389	389	370	332	217	214
Average	Experimental	367	411	409	360	333	222	227

[a]All single and multiple tooth joints failed in tooth withdrawal.
[b]Tooth withdrawal.
[c]Plate tensile failure.
[d]Plate peelback.
[e]Wood failute perpendicular to grain.
[f]Testing apparatus failure before ultimate load of joint.

The multiple teeth in a row, which were equidistant from the wood-wood juncture, all withdrew at the same time when the ultimate load was reached. A paired *t*-test showed no difference in ultimate load between the teeth in rows and in columns despite the different failure mechanism ($p < 0.05$). The average ultimate load per tooth for column and row arrangements tested against the experimental loads of the single tooth also showed no significant difference ($\alpha = 0.05$). The true strength of single-tooth joints was not reached due to their fragility. A small, but observable gap developed between the wood and plate before testing in spite of careful handling.

Complete Joint Tests

Variation in tooth size and local changes in the wood foundation modulus were averaged for joints tested with complete plates. This gave load-deflection traces a more consistent pattern than occurred in types 1, 2, and 3, where some of the teeth were removed. The general shape of the experimental and theoretical traces for test types 4 [Fig. 6(*a*)] are consistent with joint types 1, 2, and 3 except for a sizable decrease in the deflection at failure for type 4. The probable reason is the difference in the mode of failure between the single-tooth joints (types 1, 2, 3) and the complete joint (type 4). For type 4, specimens 1 and 2 exhibited joint failure by tooth withdrawal, specimens 3 and 5 failed by truss-plate tensile rupture, and testing of specimen 4 was terminated because the testing apparatus failed.

The theoretical model slightly underestimates initial joint stiffness for teeth edge bearing parallel to grain [Fig. 6(*b*)]. Although the theoretical and experimental ultimate loads are close, the shape of the deformation curves differs, mainly due to the determination of the foundation modulus. The loading head used for determination of foundation modulus with tooth edge bearing was rectangular with one dimension being actual plate thickness and the other tooth length. However, the cross section of punched-plate teeth is somewhat crimped, causing an increase in the amount of tooth-area bearing on the wood. The geometry and nonrectangular shape of the tooth in edgewise orientation increases the bearing area, especially at high load levels. Also, the somewhat sharp edges of the teeth cut wood fibers before wood crushing occurred, resulting in rapid failure.

Teeth orientated on edge are more resistant to rotation at their junction to the plate than are flat teeth. As loading approached collapse in type 5, the moment at the tooth junction was transferred into the plate, causing the plate to deform and rotate. Teeth furthest from the wood-wood contact withdrew, increasing the moment in the remaining teeth, which caused a chain reaction that culminated in failure.

The traces for joint type 6 shows trends similar to those of type 7 [Figs. 6(*c*) and 6(*d*)]. The edgewise orientation of teeth for type 7 had less effect than for type 5 joints because splitting did not occur when tooth edges were bearing perpendicular to grain.

The theoretical model for elbow joints accurately predicts behavior at low load levels [Fig. 6(*e*)]. However, it deviates at near-failure loads when teeth farthest from the center of rotation reach their carrying capacity. The outer teeth cannot carry the additional load, resulting in partial tooth withdrawal and plate buckling, which was not included in the model.

Table 3 compares the theoretical and experimental failure loads for joint types 4, 5, 6, and 7. The strength of joint type 4 was generally governed by tooth-withdrawal resistance; the model predicts the failure load of specimens 1 and 2 with sufficient accuracy, but is less accurate for specimens 3 and 5

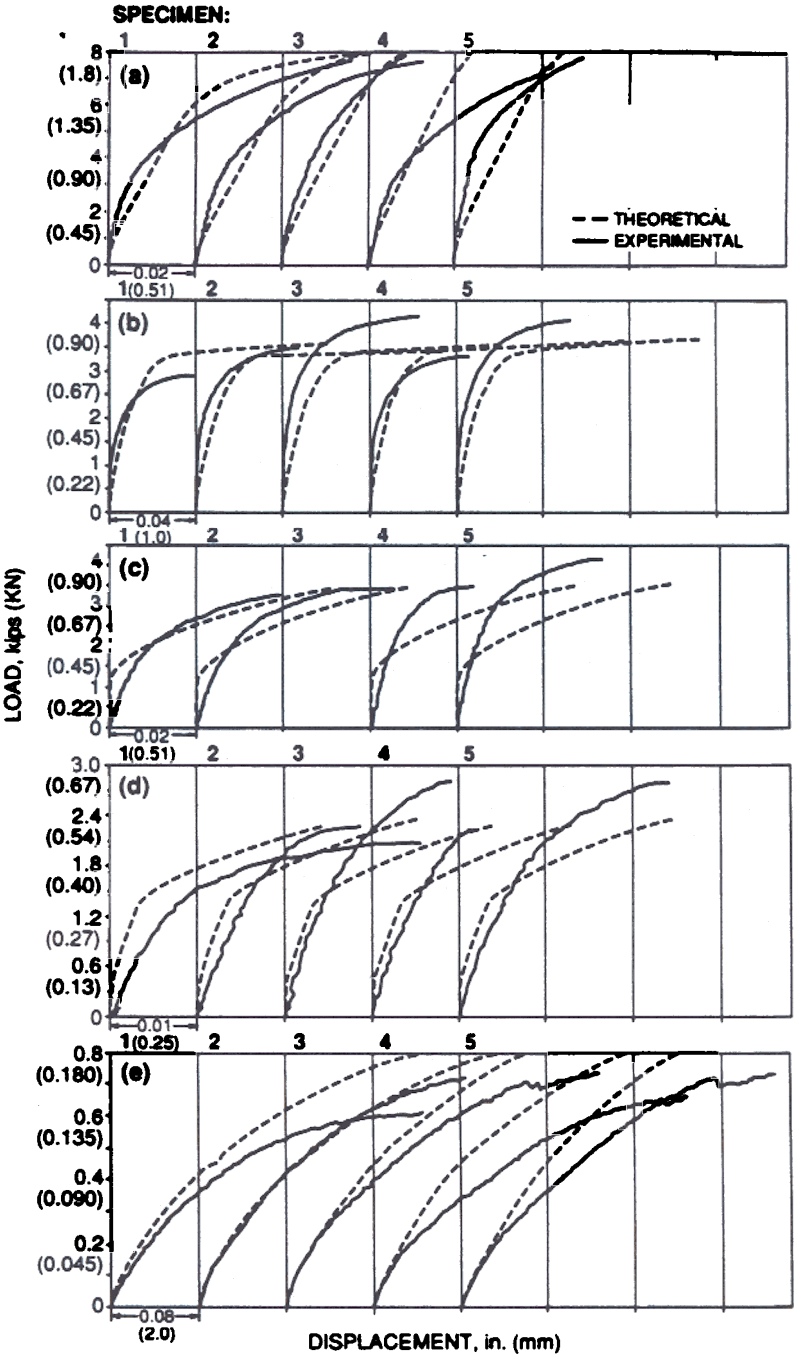

FIG. 6. Experimental versus Theoretical Traces of Slip for Joint: (*a*) Type 4; (*b*) Type 5; (*c*) Type 6; (*d*) Type 7; (*e*) Type 8

due to plate failure. Part of the inaccuracy is due to the selection of the coefficient of friction. This coefficient is the mean value selected from a study on nailed joints; the use of the mean value did not account for variability. In addition, the coefficient does not take into account the collapsed wood around the tooth, which may differ from that around the nail.

Specimens of joint type 5 with teeth edges bearing perpendicular to grain all failed in withdrawal. Although a paired *t*-test showed no difference between the theoretical and experimental withdrawal loads at the 5% significance level, the model appears to slightly underestimate the ultimate withdrawal load. This may be due to support fixity moment at the tooth base, which caused large deformations in the plate. However, other factors may be involved, such as inaccurate estimate and large variability in the foundation modulus.

The failures of joint types 6 and 7 were characterized by wood failure in tension perpendicular to grain prior to tooth withdrawal or excessive wood-bearing deformation. Because failure load was based on tooth withdrawal rather than wood failure, the theoretical failure load was overestimated. Tooth withdrawal did occur, but only after wood failure.

Conclusions

Implementation of a linear step-by-step loading procedure assisted with representation of nonlinear response of the foundation. Theoretical analysis based on a model developed by applying Runge-Kutta numerical analysis accurately predicted the load-displacement traces and ultimate load for truss-plate joints considering grain orientations and plate geometries. For single- and multiple-teeth face bearing on end grain, similar load-displacement curves and ultimate per-tooth loads were observed. Failure modes for complete joint tests varied with tooth orientation and grain direction; teeth face bearing parallel to grain failed by tooth withdrawal or plate tensile failure, teeth edge bearing parallel to grain failed by plate peel back, and teeth bearing perpendicular to grain failed in the wood in tension perpendicular to grain.

The analysis presented uses the fundamentals of mechanics to define the entire load-displacement trace of truss-plate joints and as such offers the designer added information regarding component performance. The analysis also allows the researcher to conduct rapid parametric studies and to investigate the elastic curve of a connector embedded in wood. The theory is general in nature and can be used to model any barlike timber connector that is embedded in a wood substrate.

Acknowledgments

This is paper 2638 of the Forest Research Laboratory, Oregon State University. The technical assistance of Dr. Robert Leichti is gratefully acknowledged.

Appendix I. References

Atherton, J. C. (1982). "Model for the prediction of nail withdrawal stiffness," MS thesis, Oregon State University, Corvallis, Oreg.

Beedle, L. S. (1958). *Plastic design of steel frames*. John Wiley and Sons, Inc., New York, N.Y.

Foschi, R. O. (1974). "Load-slip characteristics of nails." *Wood Sci.*, 7(1), 69–76.

Foschi, R. O. (1977a). "Analysis of wood diaphragms and trusses. Part I: diaphragms." *Can. J. Civ. Eng.*, 4, 345–352.
Foschi, R. O. (1977b). "Analysis of wood diaphragms and trusses. Part II: truss-plate connections." *Can. J. Civ. Engr.*, 4, 353–362.
Foschi, R. O. (1979). "Truss plate modeling in the analysis of trusses." *Proc. Metal Plate Wood Truss Conf.*, Forest Products Research Society, 88–97.
Foschi, R. O., and Bonac, T. (1977). "Load-slip characteristics for connections with common nails." *Wood Sci.*, 9(3), 118–123.
Foschi, R. O., and Longworth, J. (1975). "Analysis and design of griplam nailed connections." *J. Struct. Div.*, ASCE, 101(12), 2537–2555.
Groom, L. H. (1988). "Experimental verification and nonlinear modeling of truss-plate joints by Runge-Kutta numerical methods," PhD thesis, Oregon State University, Corvallis, Oreg.
Hetényi, M. (1946). *Beams on elastic foundation: theory with applications in the fields of civil and mechanical engineering*. The University of Michigan Press, Ann Arbor, Mich.
Hirai, T. (1983). "Nonlinear load-slip relationship of bolted wood-joints with steel side-members II." *J. Japan Wood Res. Society*, Tokyo, Japan, 29(12), 839–844.
Hirai, T. (1985). "Nonlinear load-slip relationship of bolted wood-joints with steel side-members III. *J. Japan Wood Res. Society*, 31(3), 165–170.
Hornbeck, R. W. (1985). *Numerical methods*. Quantum Publishers, New York, N.Y.
Kuenzi, E. W. (1953). "Theoretical design of a nailed or bolted joint under lateral load." *Forest Products Lab. Report No. 1951*, USDA Forest Service, Forest Products Laboratory, Madison, Wis.
"Methods of test for evaluation of truss plates used in lumber joints." (1980). *CSA Standard S347-M1980*, Canadian Standards Association, Ottawa, Ont.
Shigley, J. E. (1977). *Mechanical engineering design*. McGraw-Hill, Inc., New York, N.Y.
Tsujino, T., and Hirai, T. (1983). "Nonlinear load-slip relationship of bolted wood-joints with steel side-members I." *J. Japan Wood Res. Society.*, 29(12), 833–838.
Wilkinson, T. L. (1971). "Theoretical lateral resistance of nailed joints." *J. Struct. Div.*, ASCE, 97(5), 1399–1406.

Appendix II. Notation

The following symbols are used in this paper:

A, B = nonlinear regression coefficients;
b = tooth height;
d_2, d_2, d_3 = deflection limits;
E = tooth modulus of elasticity;
I_x = tooth moment of inertia at point x;
i = interval number;
k = foundation modulus;
k_1, k_2, k_3, k_4 = linear foundation moduli defined by deflection limits;
L = tooth length;
M = moment;
N = axial load;
n = number of Runge-Kutta intervals;
P = lateral load;
q = Runge-Kutta coefficients;
V = shear;
$\bar{x}$, $\bar{y}$ = truss plate center of rotation;

x = Cartesian coordinate;
y = tooth displacement
ΔP = incremental load;
Δx = interval length; and
μ = friction coefficient.